

2-23-2026

## Synthesis, Characterization, and Anticancer Activity Study of New Curcumin Analogues against MDA-MB 231 Breast Cancer Cell Line

Ola A. A. Odah

*Department of Pharmaceutical Chemistry, Collage of Pharmacy, University of Basrah, Basrah, Iraq,*  
olaodah75@gmail.com

Rita S S. Elias

*Department of Pharmaceutical Chemistry, Collage of Pharmacy, University of Basrah, Basrah, Iraq,*  
Rita.elias@uobasrah.edu.iq

Shaker A. N. N. Al-Jadaan

*Department of Pharmaceutical Chemistry, Collage of Pharmacy, University of Basrah, Basrah, Iraq,*  
shakeraljadaan2@gmail.com

Follow this and additional works at: <https://bsj.uobaghdad.edu.iq/home>

---

### How to Cite this Article

Odah, Ola A. A.; Elias, Rita S S.; and Al-Jadaan, Shaker A. N. N. (2026) "Synthesis, Characterization, and Anticancer Activity Study of New Curcumin Analogues against MDA-MB 231 Breast Cancer Cell Line," *Baghdad Science Journal*: Vol. 23: Iss. 2, Article 12.  
DOI: <https://doi.org/10.21123/2411-7986.5204>

This Article is brought to you for free and open access by Baghdad Science Journal. It has been accepted for inclusion in Baghdad Science Journal by an authorized editor of Baghdad Science Journal.



## RESEARCH ARTICLE

# Synthesis, Characterization, and Anticancer Activity Study of New Curcumin Analogues against MDA-MB 231 Breast Cancer Cell Line

Ola A. Odah<sup>1</sup>\*, Rita S Elias<sup>2</sup>, Shaker A. N. Al-Jadaan<sup>3</sup>

Department of Pharmaceutical Chemistry, Collage of Pharmacy, University of Basrah, Basrah, Iraq

## ABSTRACT

Synthesis of six new curcumin analogues was performed through condensation reaction of 3-methyl-2, 4-pentandione with substituted aromatic aldehyde derivatives and boron oxide in the presence of trimethylborate and butylamine. The reaction was carried out under ultrasonic irradiation. The synthesized compounds were identified using <sup>1</sup>H-, <sup>13</sup>C-NMR, FT-IR spectroscopy, and electron impact mass spectrometry. The Swiss ADME website was used to predict the physicochemical properties of the new compounds using computational techniques like ADME studies. All produced compounds, according to this study, complies with the Lipinski rule of five. The microculture tetrazolium (MTT) assay was utilized to assess the investigated compounds, in vitro anticancer activity against the human breast cancer cell line MDA-MB 231. The results showed that compounds 6 and 2, with IC<sub>50</sub> values of 47.78 and 111.8 μg/ml respectively, had potent anticancer activity compared to curcumin with IC<sub>50</sub> value of 125.5 μg/ml.

**Keywords:** Anticancer activity, Curcumin, Lipinski rule, Microculture tetrazolium assay, Ultrasonic irradiation

## Introduction

Natural Curcumin is a polyphenolic phytochemical compound derived from the root of rhizome *Curcuma longa*.<sup>1,2</sup> The three main curcuminoids found in turmeric are curcumin, demethoxycurcumin, and bisdemethoxycurcumin. It was first recognized by Vogel in 1815 as the main component of turmeric and it was further isolated in 1842.<sup>3,4</sup> Curcumin unsaturated  $\alpha$ - $\beta$ -diketones are generally found in nine distinct forms because of cis-trans isomerism and keto-enol tautomerism.<sup>5</sup> The Keto-enol tautomerism refers to the exchange of a proton between two constitutional isomers: keto and enol.<sup>2</sup>

Curcumin exhibits various pharmacological actions with different mechanisms of actions such as antibacterial,<sup>6</sup> anti-inflammatory,<sup>7</sup> antioxidant,<sup>8</sup> and anticancer.<sup>9,10</sup> Despite these benefits, it has many drawbacks when used as a drug; because it is poor

drug properties such as poor aqueous solubility, instability (highly pH-dependent), poor absorption, low distribution, and rapid metabolism.<sup>11,12</sup> The traditional remedy curcumin has been studied for years for its potential as an anticancer and chemopreventive agent.<sup>13</sup>

Breast carcinoma is one of the most common types of the disease. With 23 percent of cancer cases occurring in women, it is a highly variable illness in terms of both histology and molecular levels.<sup>14</sup> Based on gene expression profiling, six different subtypes have been identified, the MDA-MB-231 is a particularly aggressive and invading breast cancer cell line that exhibits ER, PR, and HER2 negative expression. Furthermore, even though numerous new drugs have been introduced to the market, patient response to therapy remains low, and drug resistance develops. Consequently, there is an urgent need to develop anticancer drugs that are less likely to cause

Received 22 May 2024; revised 4 October 2024; accepted 6 October 2024.  
Available online 23 February 2026

\* Corresponding author.

E-mail addresses: olaodah75@gmail.com (O. A. Odah), Rita.elias@uobasrah.edu.iq (R. S Elias), shakeraljadaan2@gmail.com (S. A. N. Al-Jadaan).

<https://doi.org/10.21123/2411-7986.5204>

2411-7986/© 2026 The Author(s). Published by College of Science for Women, University of Baghdad. This is an open-access article distributed under the terms of the Creative Commons Attribution 4.0 International License, which permits unrestricted use, distribution, and reproduction in any medium, provided the original work is properly cited.

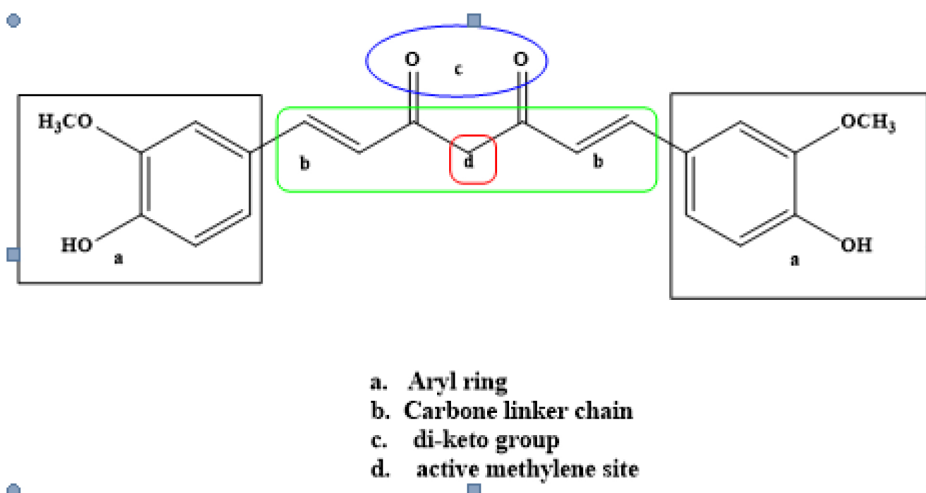


Fig. 1. Sites of modification and active functional groups of curcumin.

side effects and more effective.<sup>15</sup> To modify the molecule of curcumin it is important to study the structure of curcumin and identify the reactive sites in molecule Fig. 1.<sup>9</sup> For the heptadienedione series, the primary targets of the modifications were the aromatic ring. When the structure-activity relationship was first investigated, we focused on the substitution pattern of curcumin's aromatic ring's 3-OCH<sub>3</sub> and 4-OH groups. Removing the 4-OH groups or adding another group such as (OCH<sub>3</sub>, OC<sub>2</sub>H<sub>5</sub>, OC<sub>3</sub>H<sub>7</sub> and OC<sub>4</sub>H<sub>9</sub>) somewhat decreased or increase curcumin's anti-proliferative effects,<sup>16</sup> another modification employed active methylene position such as alpha methyl.

## Materials and methods

### Chemical and instrument

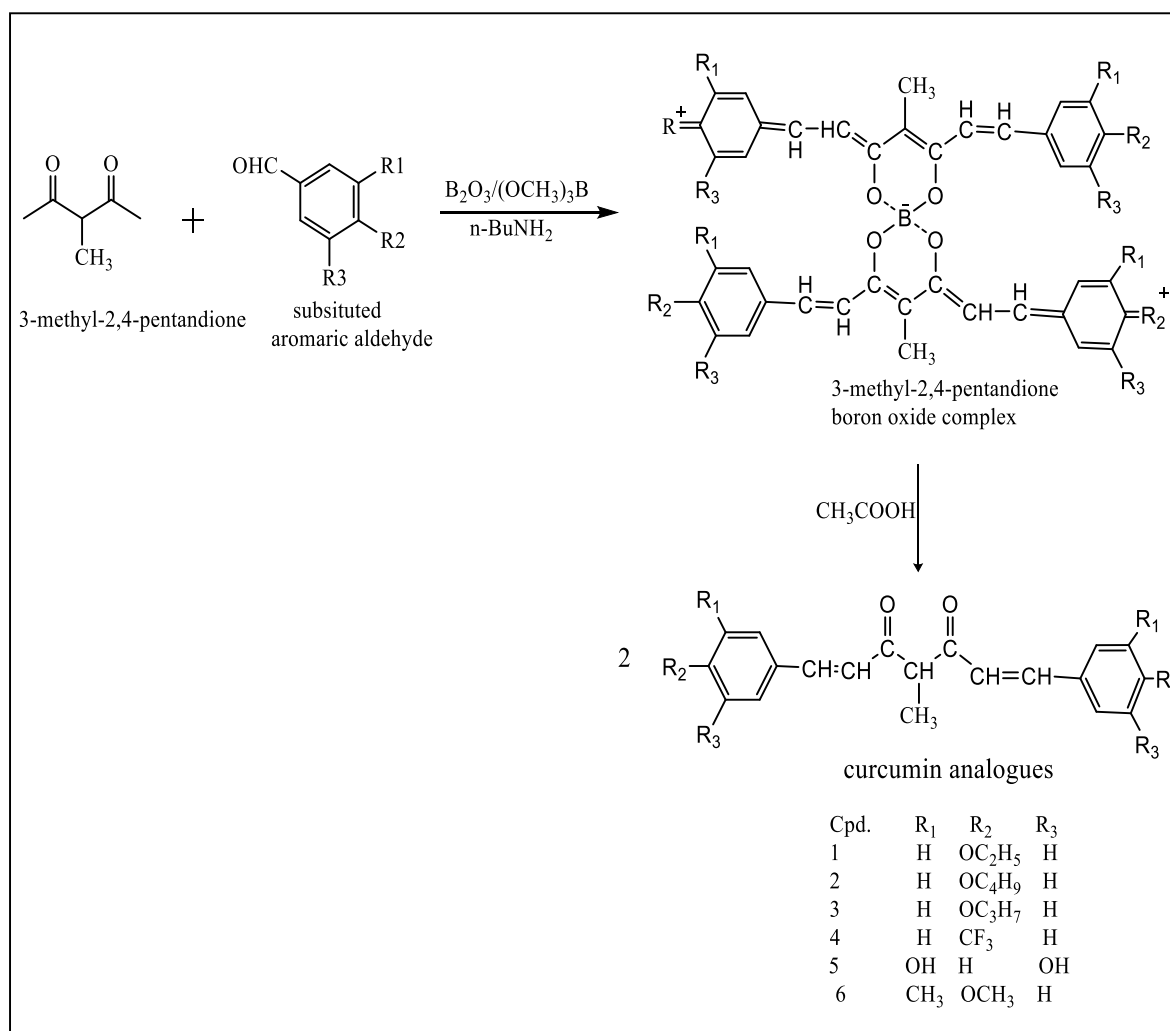
All materials are used without further purification, straight from the typical source of the most excellent quality currently in use. The ultrasonic highest energy setting (40 kHz, 500 W) was used. The melting points of the prepared curcumin analogues were measured in capillary tube using electro thermal melting point apparatus model Stuart SMP30 apparatus. Thin-layer chromatography was performed on Merck's, TLC Silica Gel 60 F254, and measuring 20 by 20 cm and with a thickness of 0.2 mm. The spot visualized by UV light. The FTIR spectra using KBr discs and expressed in the range of 4000–500 cm<sup>-1</sup> were recorded on FT-IR –84005 Shimadzu Corporation spectrophotometer at University of Basrah, College of Education for Pure Science, Department of Chemistry. Mass spectrometry of the studied compounds was done by using Agilent 5975c technologies at the University of

Tehran, Iran. The synthesized compounds were subjected to <sup>1</sup>H-NMR and <sup>13</sup>C-NMR spectroscopy at the analytical laboratory of Tehran University, College of Sciences, Department of Chemistry. The Varian (INOVA500 MHz) spectroscopy was used in DMSO-d<sub>6</sub> as a solvent, the coupling constant was specified in Hz, and the chemical shift was in part per million (ppm). The anticancer activity of synthesized compounds were done in the Malaya University, Faculty of Medicine and Pharmacology Department, by using MTT assay.<sup>17</sup>

## Experiment

### Synthesis of curcumin analogues

The general method for synthesizing certain curcumin analogues.<sup>18</sup> It includes reacting 3-methyl-2, 4-pentanedione with substituted aromatic aldehydes under ultrasonic irradiation as shown in Scheme 1. 3-methyl-2, 4-pentanedione (1.48 ml, 0.013 mol) and substituted aromatic aldehyde (0.025 mol) were added to a round-bottom flask (100 ml) along with DMF (6 ml), tri-methyl borate (2 ml), and boron oxide (0.9 g, 0.013 mol) and the mixture were exposed to ultrasonication at 80°C for ten minutes then adding the butyl amine (0.6 ml) to the round. The reaction process was monitored using TLC, and the reaction persisted for 45 minutes. After the reaction was complete, the round bottom flask was heated in a hot water bath; after adding 100 mL of warm, five percent glacial acetic acid, the reaction was stirred continuously for an hour. We used the hot water to wash and filter it. Until neutralized pH was approximately 7. The product was left to dry overnight. Column chromatography was used to separate the



**Scheme 1.** Synthesis of curcumin analogues.

**Table 1.** Physical properties of curcumin analogues 1–6.

Compound No.	Weight(g)	color	Melting point (°C)	Yield%
1	2.86	Pale reddish- orange	165–170	58
2	3.86	Pale orange	147–150	68.68
3	3.038	Yellow	154–160	57.62
4	3.306	Pale yellow	156–159	59.94
5	0.33	Yellow	243–246	4.86
6	2.65	Yellow	166–171	54.19

dried products on silica (200–300 mesh) eluted with mixture of chloroform and ethanol, ethanol solvent was used for recrystallization.

## Results and discussion

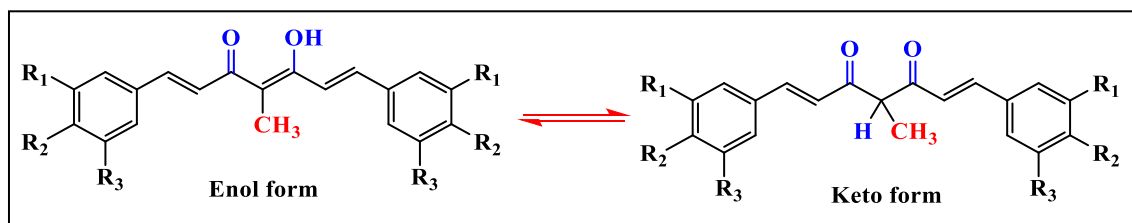
The physical properties of synthesized compounds are summarized in Table 1.

### Mass spectrometry of curcumin analogues 1–6

The mass spectral data of the compounds (1–6), are gathered in Table 2, and the mass spectra are shown in (suppl. 1–6). Electron Ionization technique is used to record the spectra of the studied molecules. From these spectra the molecular ion peaks were determined for compounds, which are equal to molecular weight of synthesis compounds.

**Table 2.** Mass spectral data of the compounds (1–6).

Compound No.	Chemical formula	Molecular weight	Molecular ions (m/z)	IUPAC Name
1	C <sub>24</sub> H <sub>26</sub> O <sub>4</sub>	378.47	378.3	(1E,6E)-1,7-bis(4-ethoxyphenyl)-4-methylhepta-1,6-diene-3,5-dione
2	C <sub>28</sub> H <sub>34</sub> O <sub>4</sub>	434.58	435.4	(1E,6E)-1,7-bis(4-butoxyphenyl)-4-methylhepta-1,6-diene-3,5-dione
3	C <sub>26</sub> H <sub>30</sub> O <sub>4</sub>	406.52	406.3	(1E,6E)-4-methyl-1,7-bis(4-propoxyphenyl) hepta-1,6-diene-3,5-dione
4	C <sub>22</sub> H <sub>16</sub> F <sub>6</sub> O <sub>2</sub>	426.36	426.3	1E,6E)-4-methyl-1,7-bis(4-(trifluoromethyl) phenyl)hepta-1,6-diene-3,5-dione
5	C <sub>20</sub> H <sub>18</sub> O <sub>6</sub>	354.36	354.1	(1E,6E)-1,7-bis(3,5-dihydroxyphenyl)-4-methylhepta-1,6-diene-3,5-dione
6	C <sub>24</sub> H <sub>26</sub> O <sub>4</sub>	378.47	378.3	(1E,6E)-1,7-bis(4-methoxy-3-methylphenyl)-4-methylhepta-1,6-diene-3,5-dione

**Scheme 2.** The keto-enol Tautomerization of curcumin analogue.

### FT-IR spectroscopy of curcumin analogues 1–6

FTIR spectra of curcumin analogues which were prepared from appropriate benzaldehyde with absorption bands at 1687–1786 cm<sup>-1</sup> are attributed to the carbonyl groups of aldehyde.<sup>19</sup> This band disappeared from the spectra of curcumin analogues, their carbonyl band appear at 1617–1629 cm<sup>-1</sup> due to the formation of the intra-hydrogen bonded.<sup>20,21</sup> The aromatic(C-H) stretches are responsible for the bands in the infrared spectrum at 3074–3076.4 cm<sup>-1</sup> weak band.<sup>22</sup> C=C stretching band appeared as strong band at 1600–1500 cm<sup>-1</sup> which are attributed to the stretching vibrations of their C=C.<sup>21</sup> The weak broad band appeared in range 3200–2500 cm<sup>-1</sup> for enolic ν(OH) this range is not very accurate due to overlapping with C-H stretching in this region.<sup>22</sup> The aliphatic C-H stretches bands have been observed as weak band in the infrared spectra (2800–3000) cm<sup>-1</sup>. The FTIR spectrum of compound 5 showed very clear sharp bands in rang 3500–3200 cm<sup>-1</sup> which are attributed to the stretching vibrations of their phenolic OH<sup>23</sup> (suppl.7–12).

### <sup>1</sup>H-NMR spectra of curcumin analogues 1–6

<sup>1</sup>H-NMR spectra of compounds (1–6) (suppl. 13–18) had two peaks at 2.5 ppm and 3.3 ppm that were related to the solvent DMSO-d<sub>6</sub> and water respectively. The presence of both the β-diketone form and the keto-enol tautomer for curcumin analogs in solvent DMSO-d<sub>6</sub> has been clearly established.<sup>2</sup> In solution, both tautomers are present at the same time as shown in Scheme 2.

<sup>1</sup>H-NMR spectra of curcumin analogs require the tautomerism of molecules in keto-enol form. This spectrum shows singlet signal at 17.66 ppm corresponding mainly to the enolic proton. Its position downfield has been attributed to the combined effect of strong intramolecular hydrogen bonds and the conjugation through the system.<sup>24</sup> The phenolic protons (OH) which can be observed at 9–9.5 ppm disappear in all compounds with the exception of compounds 5, while the signals at 4.58 ppm as quartet refer to the methine (CH) keto form. The spectrum showed triplet and quartet signals at 4.07 ppm and 1.33 ppm referred to the 2 methyl and 2 methylene proton of the alkoxy group. The aromatic and olefinic protons signals developed as multiplet near 6.87–7.74 ppm. At 2.18 ppm, the α-methyl proton of enol form can be observed as a singlet, while the α-methyl proton of keto form signals appeared as doublet at 1.28 ppm with *J* coupling constant 7 Hz. The interaction of keto and enolic protons determined how its integrates are challenging.<sup>25</sup>

### <sup>13</sup>C-NMR spectra of compounds 1–6

<sup>13</sup>C-NMR spectra of compounds 1–6 were shown in Figs. 2 to 7. Using <sup>13</sup>C-NMR the presence of both the β-diketone form and the keto-enol tautomer for curcumin analogs in solvent DMSO-d<sub>6</sub> has been clearly established as shown in Scheme 3.<sup>25</sup>

These spectra had signals at 40 ppm that related to the solvent DMSO-d<sub>6</sub>. The <sup>13</sup>C-NMR spectra for the β-diketone tautomer suggest that carbonyl carbon in the keto-enol form is slightly less deshielded than in the β-diketone form.<sup>26</sup> In <sup>13</sup>C-NMR

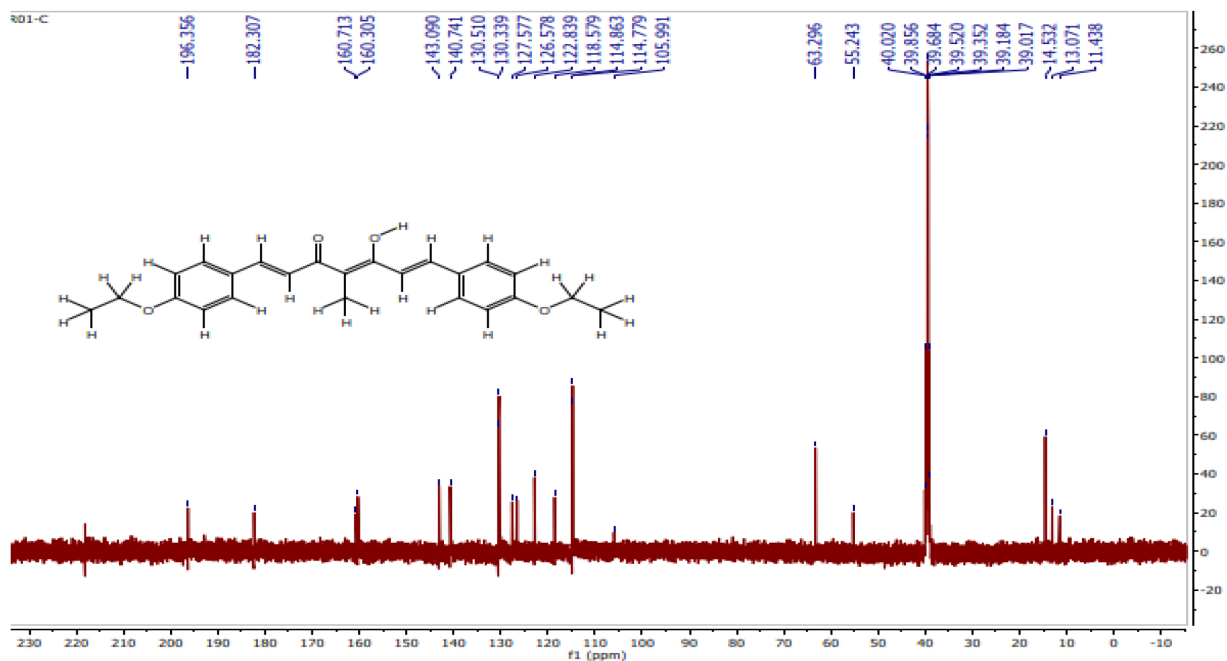


Fig. 2. The <sup>13</sup>C-NMR spectrum of compound (1).

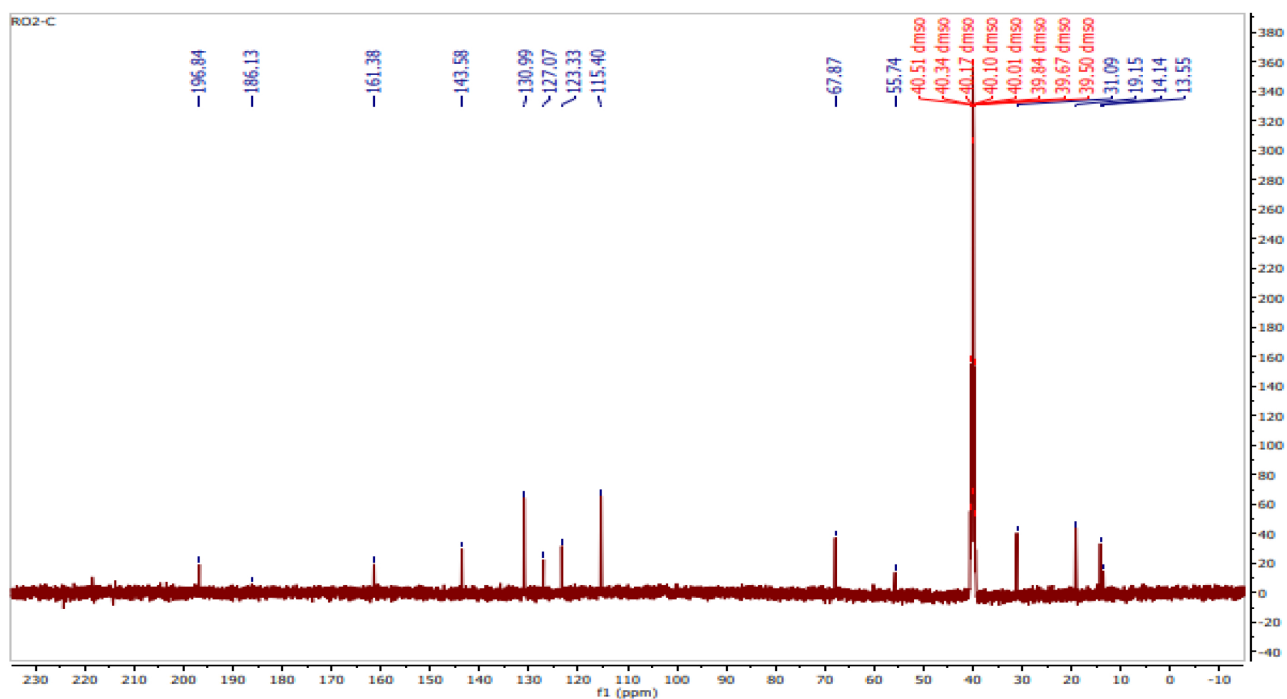


Fig. 3. The <sup>13</sup>C-NMR spectrum of compound (2).

spectra we can observed the distinctive signals as following:

- The keto carbon (C5) signal appear at 196.2–197.3 ppm while the enol carbon (C3) at 180.2–186.1ppm.<sup>25,27</sup>
- The signal at 160.3–161.4 ppm referred to aromatic carbon (C4) attached to alkoxy group,<sup>28</sup> shielded of the signal to up field when attached to trifluoromethyl group.
- The signals at 140.1–144.3 ppm referred to heptadienedione carbon (C1, C7). The signals at

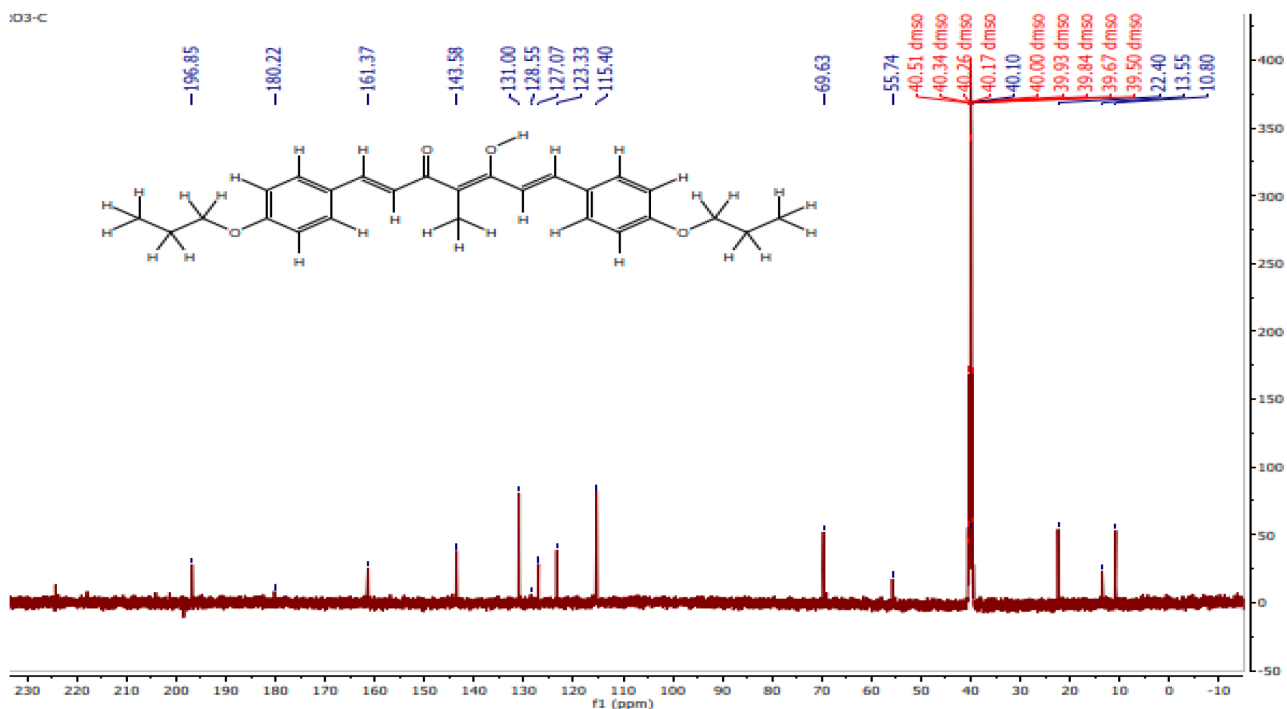


Fig. 4. The <sup>13</sup>C-NMR spectrum of compound (3).

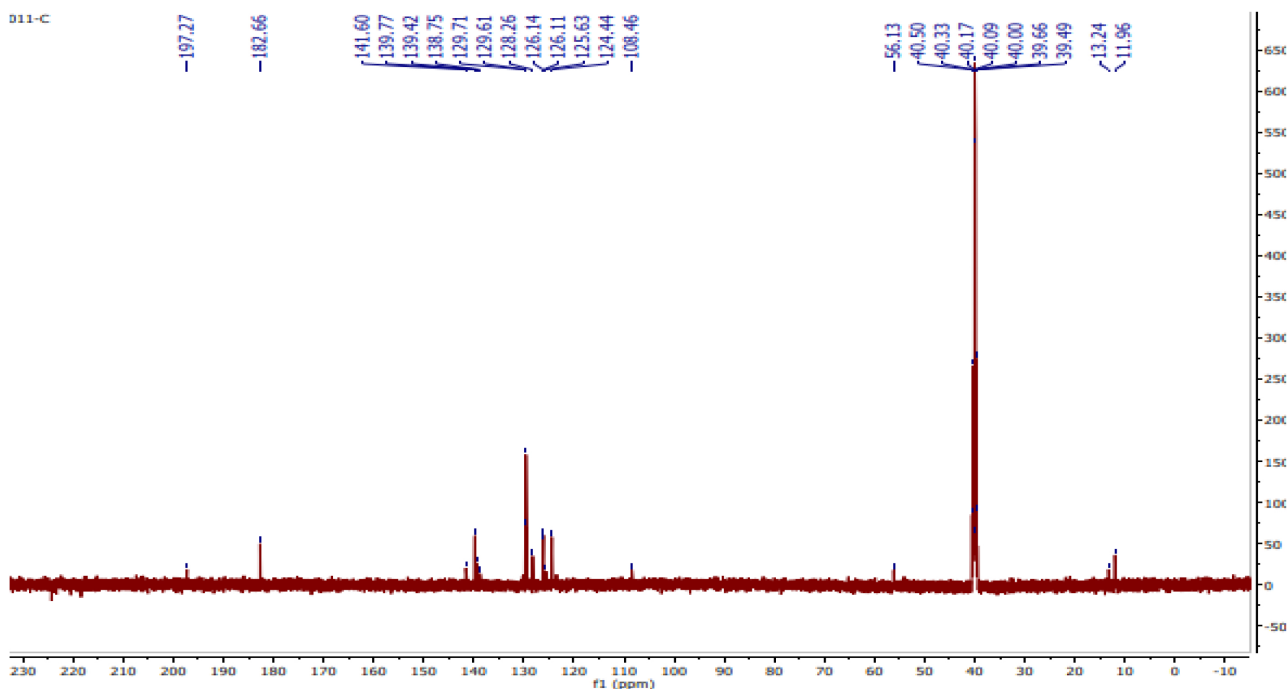


Fig. 5. The <sup>13</sup>C-NMR spectrum of compound (4).

118.6–124.4 ppm referred to heptadienedione carbon (C2, C6).<sup>25</sup>

- The alpha methyl carbon (CH<sub>3</sub>) signal appeared at 10.80–13.55 ppm.<sup>25</sup>
- The carbon CH of keto form C4 signals appeared at 69.6–55.5 ppm, while the enol form signal ap-

peared within the range 105.25–115.4 ppm. The aliphatic methyl carbon signal at 14.5 ppm and 13.1 ppm referred to keto and enol form respectively<sup>25</sup>.

- The aromatic ring carbon (C3) signal appeared at 114.9 ppm and (C5) signal at 114.8 ppm.

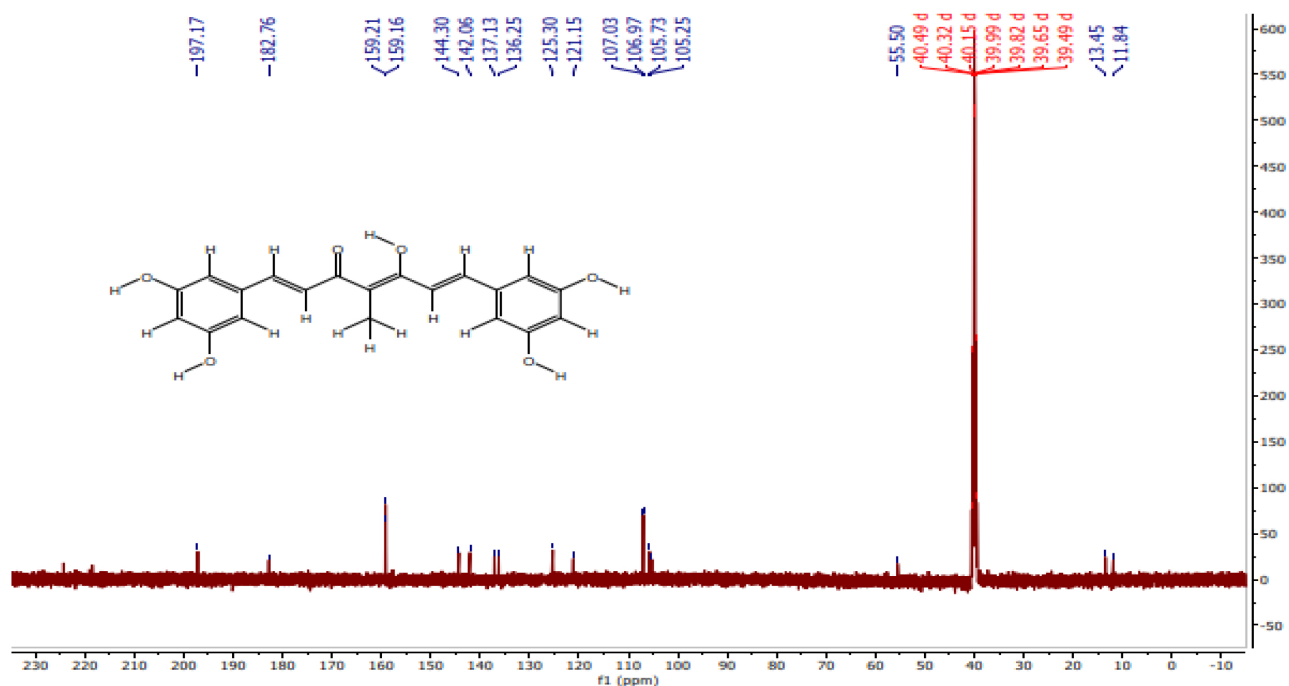


Fig. 6. The <sup>13</sup>C-NMR spectrum of compound (5).

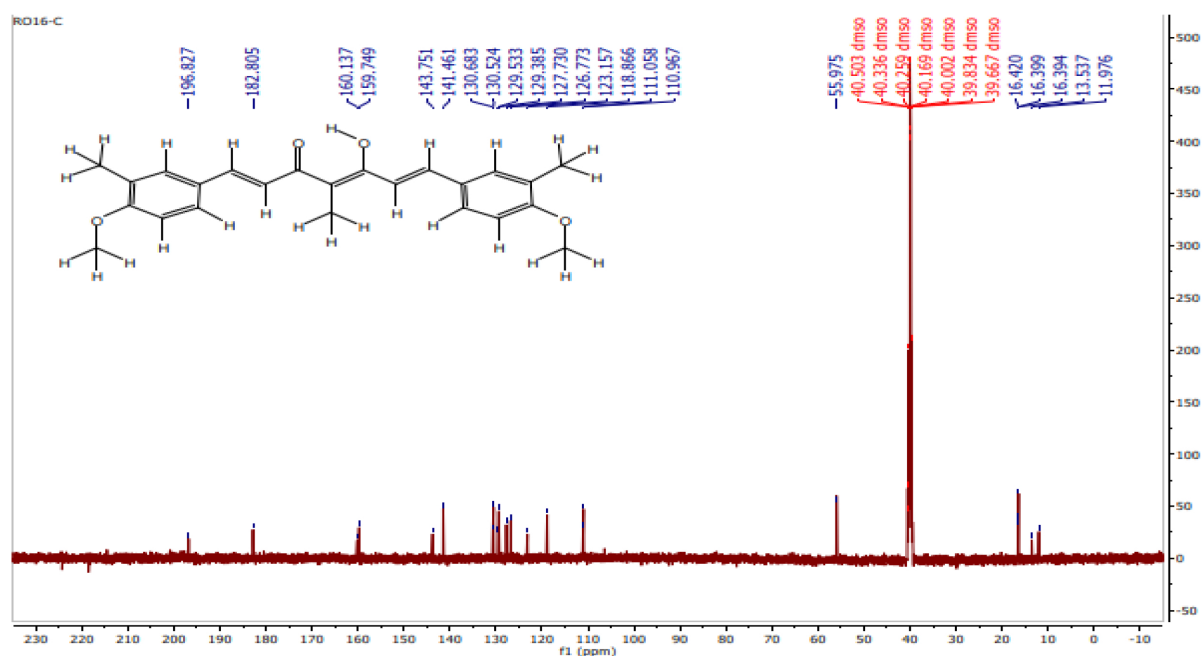
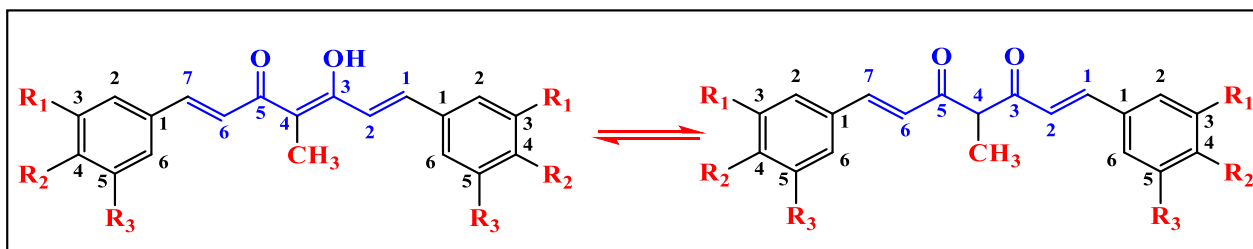


Fig. 7. The <sup>13</sup>C-NMR spectrum of compound (6).

and (C2,C6) signal at 130.5 ppm. The carbon aromatic (C1) signal appeared at 127.5 ppm.<sup>25</sup> For the compounds (4) the multiplet signal at 126.1 ppm referred to fluorinated carbon.<sup>25,29</sup>

#### *The physicochemical properties of curcumin analogues 1–6 by lipinski's rule of five*

The physicochemical properties of the studies compounds were computed by the Swiss ADME website.



**Scheme 3.** The keto-enol Tautomerization of curcumin analogue.

**Table 3.** Lipinski properties obtained for the curcumin analogues.

Compound No.	Mol.wt.(g/mol)	NRB	NHBD	NHBA	TPSA( $\text{\AA}^2$ )	Log p	Lipinski's Rule of Five Violation
1	378.46	9	1	4	55.76	4.21	0
2	434.57	13	1	4	55.76	5.19	0
3	406.51	11	1	4	55.76	4.49	0
4	426.35	7	1	8	37.30	3.43	1
5	354.35	5	5	6	118.22	1.74	0
6	378.46	7	1	4	55.76	4.02	0

Mol. wt.: molecular weight, NRB: number of rotatable bonds, NHBA: number of hydrogen bond acceptors, NHBD: number of hydrogen bond donors, TPSA: topological polar surface area, Log P: logarithm partitioning coefficient.

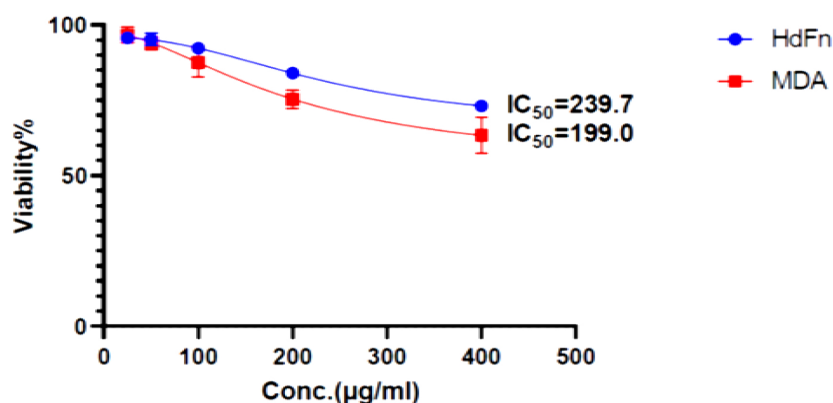


**Fig. 8.** Impact of compound (1) at various concentrations on the cell viability percentage.

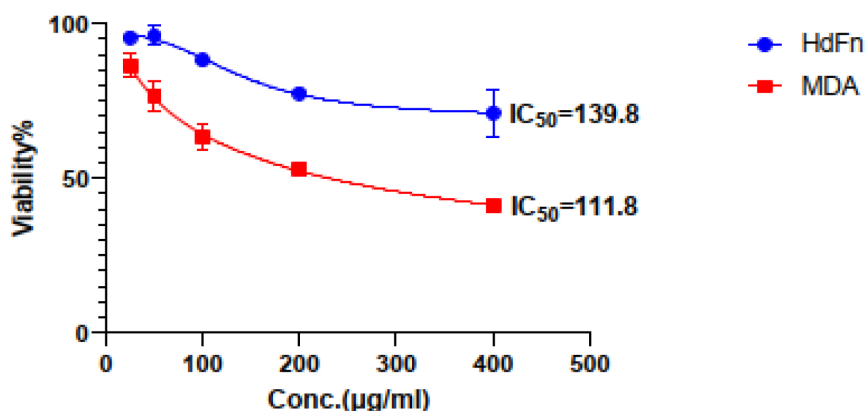


**Fig. 9.** Impact of compound (2) at various concentrations on the cell viability percentage.

It is freely available URL (<http://www.swissadme.ch/>) was applied to computed ADME, the pharmacokinetic, and other drug-like properties by drawing

the chemical structure and entering SMILE.<sup>30</sup> All the results for Lipinski properties obtained for curcumin analogues are shown in Table 3. According to the rule

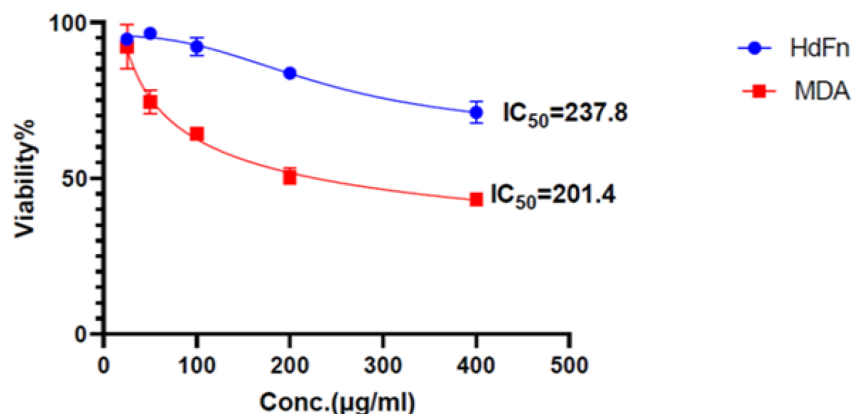


Fig. 10. Impact of compound (3) at various concentrations on the cell viability percentage.

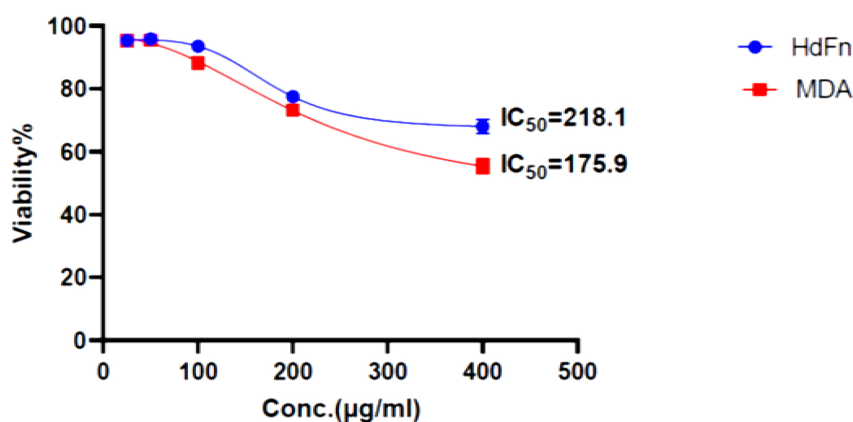


Fig. 11. Impact of compound (4) at various concentrations on the cell viability percentage.

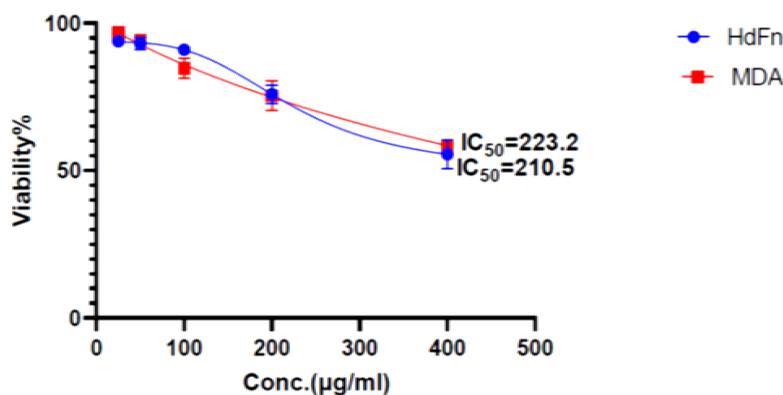


Fig. 12. Impact of compound (5) at various concentrations on the cell viability percentage.

of five, there should be equal or fewer than five hydrogen bond donors, fewer than ten Hydrogen bond acceptors, a molecular weight (M.wt.) of below 500, and a logarithm partitioning coefficient (Log p) of equal or less than five for there to be good absorption or penetration.<sup>31</sup> The results showed that the computed molecular weight for compounds ranges from 354.35 to 434.57 g/mol. The results showed

the number of hydrogen bond donors for compounds in the range 1–5 and the number of hydrogen bond acceptors for compounds in the range 1–8. The recently developed PSA calculating method is known as TPSA (topological PSA).<sup>32</sup> For a molecule to penetrate a cell membrane, its PSA must be  $< 140 \text{ \AA}^2$  and must be less than  $90 \text{ \AA}^2$  to pass through the blood-brain barrier.<sup>32,33</sup> The results that show the polar

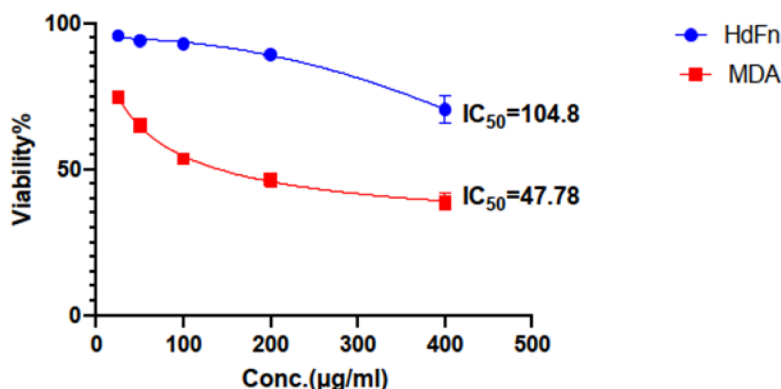


Fig. 13. Impact of compound (6) at various concentrations on the cell viability percentage.

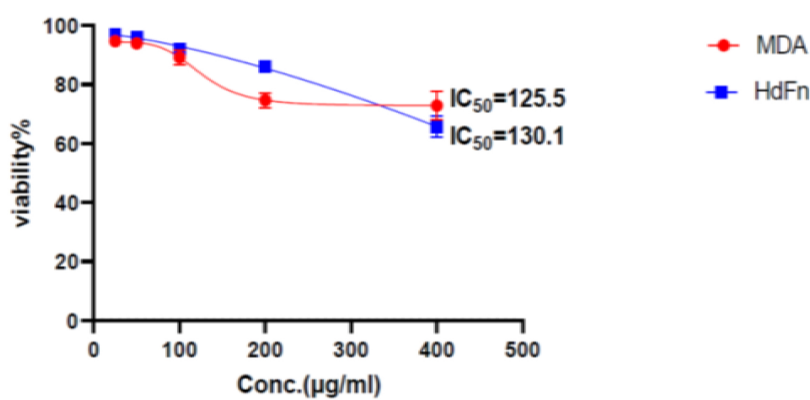


Fig. 14. Impact of compound (7) at various concentrations on the cell viability percentage.

Table 4. The  $IC_{50}$  and SI of curcumin and its analogues.

Compound No.	HdFn ( $IC_{50}$ ) $\mu$ g/ml	MDA-MB231 ( $IC_{50}$ ) $\mu$ g/ml	selectivity index (SI)
1	239.7	199.0	1.2
2	139.8	111.8	1.3
3	237.8	201.4	1.2
4	218.1	175.9	1.2
5	223.2	210.5	1.06
6	104.8	47.78	2.2
curcumin	130.1	125.5	1.03

surface area of compounds in ranges from 37.3–55.76 except compound 5 have TPSA 118.22  $\text{\AA}^2$ . The compound is not considered orally active if two or more of these characteristics do not match the requirements of rule five. If a molecule fits Lipinski's rule of five, it is classified as a drug.<sup>34</sup>

#### *In vitro* anticancer assay of curcumin analogues

The studies compounds were preliminary tested for their *in vitro* anticancer activity against the human breast cancer cell line MDA-MB231 using the MTT assay. This assay is widely used to screen for cytotoxic compounds during the development of chemotherapy.<sup>35</sup> That uses colorimetric techniques based on mitochondrial dehydrogenase activity measurement to estimate the amount of viable cells. 3-(4,5-dimethylthiazol-2-yl)-2,5-diphenyltetrazolium bromide yellow colored is reduced by dehydrogenase in living cells to produce a crystals purple colored formazan dye, and subsequent solvation of the crystals with a suitable solvent and measuring their absorbance of light at 570 nm. The cytotoxic activity of curcumin derivatives 1–6 were estimated *in vitro* via MTT assay against breast cancer cell lines MDA-MB231. The half maximal Inhibitory Concentration ( $IC_{50}$ ) was determined based on the dose–response curve created after finding the percent of the cell death at several concentrations of the composites as shown in Figs. 8

metric techniques based on mitochondrial dehydrogenase activity measurement to estimate the amount of viable cells. 3-(4,5-dimethylthiazol-2-yl)-2,5-diphenyltetrazolium bromide yellow colored is reduced by dehydrogenase in living cells to produce a crystals purple colored formazan dye, and subsequent solvation of the crystals with a suitable solvent and measuring their absorbance of light at 570 nm. The cytotoxic activity of curcumin derivatives 1–6 were estimated *in vitro* via MTT assay against breast cancer cell lines MDA-MB231. The half maximal Inhibitory Concentration ( $IC_{50}$ ) was determined based on the dose–response curve created after finding the percent of the cell death at several concentrations of the composites as shown in Figs. 8

to 14. The anticancer activity of compounds is categorized into three groups based on their cell growth inhibition; active  $IC_{50} < 20\mu\text{g/ml}$ , moderate activity  $IC_{50} 20\text{--}100\mu\text{g/ml}$  and inactive  $IC_{50} > 100\mu\text{g/ml}$ .<sup>36</sup>

The selectivity index (SI) is known as the ratio of the tested compounds cytotoxicity in normal cells ( $IC_{50}$  HdFn  $\mu\text{g/ml}$ ) versus cancer cells ( $IC_{50}$  MDA-MB231). Compounds with anticancer specificity indicated by SI values higher than 1.0, while compounds with significantly higher SI values than 1.0 are highly selective.<sup>37</sup> All synthesized compounds exhibited cytotoxicity with  $IC_{50}$  assumed in a range of 47.78–210.5  $\mu\text{g/mL}$  as shown in Table 4.

The cytotoxic activity of curcumin derivatives was estimated and it was found that compound 6 with  $IC_{50}$  47.78  $\mu\text{g/ml}$  and with SI 2.2 which have moderate anticancer activity and highly selectivity against MDA-MB231 and more potent anticancer activity in comparison to curcumin whereas compound 2 with  $IC_{50}$  111.8  $\mu\text{g/ml}$  and SI 1.3 was considered as specific anticancer activity against MDA-MB231 and has more anticancer activity in comparison to curcumin with  $IC_{50}$  equal to 125.5  $\mu\text{g/ml}$  and SI 1.03.

## Conclusion

Curcumin analogues 6 was characterized by highly selective anticancer activity against MDA-MB-231, the most potent anticancer agent observed, with  $IC_{50}$  of 47.78  $\mu\text{g/mL}$  and SI of 2.2, the methoxy group at the para position of the aromatic ring and a methyl group at the meta position led to increase in the lipophilicity of compound 6 and increase in cytotoxicity. Compound 2 with  $IC_{50}$  of 111.8  $\mu\text{g/mL}$  and SI of 1.3 has specific anticancer activity against MDA-MB231 and has higher anticancer activity and selectivity against MDA-MB231 compared to curcumin with  $IC_{50}$  of 125.5  $\mu\text{g/mL}$  and SI of 1.03.

## Authors' declaration

- Conflicts of Interest: None.
- We hereby confirm that all the figures and tables in the manuscript are ours. Furthermore, figures and images, that are not ours, have been included with the necessary permission for republication, which is appended to the manuscript.
- No animal studies are present in the manuscript.
- Authors signed on ethical consideration's approval.
- Ethical Clearance: The project was approved by the local ethical committee at University of Basrah.

## Authors' contribution statement

The present study's topic was suggested and organized by R. S. E. and S. A. N. while O. A. O developed and carried out the experiments and wrote the manuscript. All authors participated in the analysis, discussion and contributed to the final manuscript.

## Supplementary materials

Supplementary materials are available at [https://bsj.uobaghdad.edu.iq/cgi/viewcontent.cgi?filename=0&article=5204&context=home&type=additional&preview\\_mode=1](https://bsj.uobaghdad.edu.iq/cgi/viewcontent.cgi?filename=0&article=5204&context=home&type=additional&preview_mode=1).

## References

1. Oluwafemi A, Ajayi O, Oseni O. Phytochemical screening, nutritional composition, and antioxidant activities of turmeric (*curcuma longa*) found in ado-ekiti, Nigeria. *J Appl Life Sci Int.* 2022;25(1):1–8. <https://doi.org/10.9734/JALSI/2022/v25i130278>.
2. Courtney CH, Krishnan VV. Keto–enol tautomerization of acetylacetone in mixed solvents by NMR spectroscopy. A physical chemistry experiment on the application of the onsager-kirkwood model for solvation thermodynamics. *J Chem Educ.* 2020;97(3):825–830. <https://doi.org/10.1021/acs.jchemed.9b00737>.
3. Sharma G, Thakur N. Curcumin—the healing herb: Properties and future prospective. *Asian J Pharm Clin Res.* 2020;13(2):4–9. <https://doi.org/10.22159/ajpcr.2020.v13i2.28929>.
4. Nelson KM, Dahlin JL, Bisson J, Graham J, Pauli GF, Walters MA. The essential medicinal chemistry of curcumin. *J Med Chem.* 2017;60(5):1620–1637. <https://doi.org/10.1021/acs.jmedchem.6b00975>.
5. Mohammadi E, Amini SM, Mostafavi SH, Amini SM. An overview of antimicrobial efficacy of curcumin-silver nanoparticles. *Nanomed Res J.* 2021;6(2):105–111. <https://doi.org/10.22034/nmrj.2021.02.002>.
6. Zheng D, Huang C, Huang H, Zhao Y, Khan MRU, Zhao H, *et al.* Antibacterial mechanism of curcumin: A review. *Chem Biodivers.* 2020;17(8):1–14. <https://doi.org/10.1002/cbdv.202000171>.
7. Chainoglou E, Hadjipavlou-Litina D. Curcumin analogues and derivatives with anti-proliferative and anti-inflammatory activity: Structural characteristics and molecular targets. *Expert Opin Drug Discov.* 2019;14(8):821–842. <https://doi.org/10.1080/17460441.2019.1614560>.
8. Shaikh SAM, Singh BG, Barik A, Balaji NV, Subbaraju GV, Naik DB, *et al.* Unravelling the effect of  $\beta$ -diketo group modification on the antioxidant mechanism of curcumin derivatives: a combined experimental and DFT approach. *J Mol Struct.* 2019;1193:166–176. <https://doi.org/10.1016/j.molstruc.2019.05.029>.
9. Rodrigues FC, Anil Kumar NV, Thakur G. Developments in the anticancer activity of structurally modified curcumin: An up-to-date review. *Eur J Med Chem.* 2019;177:76–104. <https://doi.org/10.1016/j.ejmech.2019.04.058>.
10. Muhammad S, Saba A, Khera RA, Al-Sehemi AG, Algarni H, Iqbal J, *et al.* Virtual screening of potential inhibitor against breast cancer-causing estrogen receptor alpha ( $ER\alpha$ ): molecular docking and dynamic

- simulations. *Mol Simul* 2022;48(13):1163-1174. <https://doi.org/10.1080/08927022.2022.2072840>.
11. Kharat M, Du Z, Zhang G, McClements DJ. Physical and chemical stability of curcumin in aqueous solutions and emulsions: Impact of pH, temperature, and molecular environment. *J Agric Food Chem*. 2017;65(8):1525-1532. <https://doi.org/10.1021/acs.jafc.6b04815>.
  12. Oglah MK, Mustafa YF, Bashir MK, Jasim MH, Mustafa YF. Curcumin and its derivatives: A review of their biological activities. *Syst Rev Pharm*. 2020;11(3):472-481. <https://doi.org/10.5530/srp.2020.3.60>.
  13. Salehi B, Stojanovic-Radic Z, Matejic J, Sharifi-Rad M, Anil Kumar NV, Martins N, et al. The therapeutic potential of curcumin: A review of clinical trials. *Eur J Med Chem*. 2019;163(1):527-545. <https://doi.org/10.1016/j.ejmech.2018.12.016>.
  14. Hu S, Xu Y, Meng L, Huang L, Sun H. Curcumin inhibits proliferation and promotes apoptosis of breast cancer cells. *Exp Ther Med*. 2018;16(2):1266-1272. <https://doi.org/10.3892/etm.2018.6345>.
  15. Mohammed F, Rashid-Doubell F, Taha S, Cassidy S., Fredericks S. Effects of curcumin complexes on MDA-MB-231 breast cancer cell proliferation. *Int J Oncol*. 2020;57(2):445-455. <https://doi.org/10.3892/ijo.2020.5065>.
  16. Fuchs JR, Pandit B, Bhasin D, Etter JP, Regan N, Abdelhamid D, et al. Structure-activity relationship studies of curcumin analogues. *Bioorg Med Chem Lett*. 2009;19(7):2065-2069. <https://doi.org/10.1016/j.bmcl.2009.01.104>.
  17. Ghasemi M, Turnbull T, Sebastian S, Kempson I. The MTT assay: Utility, limitations, pitfalls, and interpretation in bulk and single-cell analysis. *Int J Mol Sci*. 2021;22(23):12827. <https://doi.org/10.3390/ijms222312827>.
  18. AL-Hakiem MM, Alderawy MQ, Adnan R, Elias RS. Synthesis, characterization, and antibacterial activity study of novel curcuminoids derivatives. *Iraqi J Pharm Sci*. 2024;33(1):154-162. <https://doi.org/10.31351/vol33iss1pp154-162>.
  19. Vennila P, Govindaraju M, Venkatesh G, Kamal C. Molecular structure, vibrational spectral assignments (FT-IR and FT-RAMAN), NMR, NBO, HOMO-LUMO and NLO properties of O-methoxybenzaldehyde based on DFT calculations. *J Mol Struct*. 2016;1111:151-156. <https://doi.org/10.1016/j.molstruc.2016.01.068>.
  20. Faisal AG, Hassan QMA, Alsalm TA, Sultan HA, Kamounah FS, Emshary CA. Synthesis, optical nonlinear properties, and all-optical switching of curcumin analogues. *J Phys Org Chem*. 2022;35(10):e4401. <https://doi.org/10.1002/poc.4401>.
  21. Badran HA, Al-Maliki A, Alfahed RF, Saeed BA, Al-Ahmad A, Al-Saymari F, et al. Synthesis, surface profile, nonlinear reflective index and photophysical properties of curcumin compound. *J Mater Sci Mater Electron*. 2018;29:10890-10903. <https://doi.org/10.1007/s10854-018-9167-0>.
  22. Racz C-P, Racz LZ, Floare CG, Tomoia G, Horovitz O, Riga S, et al. Curcumin and whey protein concentrate binding: Thermodynamic and structural approach. *Food Hydrocoll*. 2023;139(5):1-18. <https://doi.org/10.1016/j.foodhyd.2023.108547>.
  23. Jayaweera HC, Siriwardane I, de Silva KN, de Silva RM. Synthesis of multifunctional activated carbon nanocomposite comprising biocompatible flake nano hydroxyapatite and natural turmeric extract for the removal of bacteria and lead ions from aqueous solution. *Chem Cent J*. 2018;12:1-14. <https://doi.org/10.1186/s13065-018-0384-7>.
  24. Tahay P, Parsa Z, Zamani P, Safari N. A structural and optical study of curcumin and curcumin analogs. *J Iran Chem Soc*. 2022;19(7):3177-3188. <https://doi.org/10.1007/s13738-022-02522-x>.
  25. Prasad D, Praveen A, Mahapatra S, Mogurampelly S, Chaudhari SR. Existence of beta-diketone form of curcuminoids revealed by NMR spectroscopy. *Food Chem*. 2021;360:130000. <https://doi.org/10.1016/j.foodchem.2021.130000>.
  26. Hansen PE. Structural studies of  $\beta$ -diketones and their implications on biological effects. *Pharma*. 2021;14(11):1-18. <https://doi.org/10.3390/ph1411189>.
  27. Khudhayer Oglah M, Fakri Mustafa Y. Curcumin analogs: Synthesis and biological activities. *Med Chem Res*. 2020;29(3):479-486. <https://doi.org/10.1007/s00044-019-02497-0>.
  28. Thaçi V, Reka AA, Ristovska N, Hoti R, Berisha A, Bogdanov J. Experimental and theoretical studies on (2E, 5E)-2, 5-bis (2-methoxybenzylidene) cyclopentanone: Structural, electrochemical, spectroscopic features, solid-state interactions, molecular docking and adsorption studies onto 2D carbon nanomaterials. *Maced J Chem Chem Eng*. 2023;42(2):175-194. <https://doi.org/10.20450/mjcee.2023.2727>.
  29. Saunders C, Khaled MB, Weaver III JD, Tantillo DJ. Prediction of 19F NMR chemical shifts for fluorinated aromatic compounds. *J Org Chem*. 2018;83(6):3220-3225. <https://doi.org/10.1021/acs.joc.8b00104>.
  30. Hussen NH. Synthesis, characterization, molecular docking, ADMET prediction, and anti-inflammatory activity of some Schiff bases derived from salicylaldehyde as a potential cyclooxygenase inhibitor. *Baghdad Sci J*. 2023;20(5):1662-1662. <https://dx.doi.org/10.21123/bsj.2023.7181>.
  31. Chen X, Li H, Tian L, Li Q, Luo J, Zhang Y. Analysis of the physicochemical properties of acaricides based on lipinski's rule of five. *J Comput Biol*. 2020;27(9):1397-1406. <https://doi.org/10.1089/cmb.2019.0323>.
  32. Haritha M, Sreerag M, Suresh CH. Quantifying the hydrogen-bond propensity of drugs and its relationship with Lipinski's rule of five. *New J Chem*. 2024;48(11):4896-4908. <https://doi.org/10.1039/D3NJ05476D>.
  33. Adejoro IA, Waheed SO, Adeboye OO, Akhigbe FU. Molecular docking of the inhibitory activities of triterpenoids of *lonchocarpus cyanescens* against Ulcer. *J Biophys Chem*. 2017;8(1):1-11. <https://doi.org/10.4236/jbpc.2017.81001>.
  34. Sampat G, Suryawanshi SS, Palled MS, Patil AS, Khanal P, Salokhe AS. Drug likeness screening and evaluation of physicochemical properties of selected medicinal agents by computer aided drug design tools. *Adv Pharmacol Pharm*. 2022;10(4):234-246. <https://doi.org/10.13189/app.2022.100402>.
  35. Alsaad H, Kubba A, Tahtamouni LH, Hamzah AH. Synthesis, docking study, and structure activity relationship of novel anti-tumor 1, 2, 4 triazole derivatives incorporating 2-(2, 3-dimethyl aminobenzoic acid) moiety. *Pharmacia*. 2022;69(2):415-428. <https://doi.org/10.3897/pharmacia.69.e83158>.
  36. Wahyuningsih TD, Suma AAT, Astuti E. Synthesis, anticancer activity, and docking study of N-acetyl pyrazolines from veratraldehyde. *J Appl Pharm Sci*. 2019;9(3):014-020. <https://doi.org/10.7324/JAPS.2019.90303>.
  37. Jihad RS, Abdul-Rida NA, Al-Shamari AMJ, Al-Masoudi NA, Saeed BA. Design, synthesis, and in-silico study of new letrozole derivatives as prospective anticancer and antioxidant agents. *Z fur Naturforsch - B* 2023;78(6):343-353. <https://doi.org/10.1515/znB-2022-0151>.

## تحضير, تشخيص ودراسة الفعالية المضادة للسرطان لنظائر الكركمين الجديدة ضد خلايا سرطان الثدي MDA-MB231

علا عبدالحسين عودة، ريتا صباح الياس، شاكِر عبد السالم نعمة الجدعان

قسم الكيمياء الصيدلانية، كلية الصيدلة، جامعة البصرة، البصرة، العراق.

### الخلاصة

تحضير ستة نظائر جديدة للكركمين من خلال تفاعل التكتيف لـ 3-ميثيل-4،2-بنتانديون مع مشتقات الأدهايد المعوضة وأوكسيد البورون وبوجود ثلاثي ميثيل بورات و بيوتيل أمين. تم تنفيذ التفاعل تحت إشعاع بالموجات فوق الصوتية باستعمال جهاز الرنين الصوتي. المركبات المحضرة تم التعرف عليها باستخدام مطيافية الرنين النووي المغناطيسي للبروتون ( $^1\text{H-NMR}$ ) والرنين النووي المغناطيسي للكربون ( $^{13}\text{C-NMR}$ ) وطيف الأشعة تحت الحمراء (FTIR) ومطيافية الكتلة التصادمية للإلكترون (MS). تم استخدام موقع (ADME) السويسري للتنبؤ بالخصائص الفيزيائية والكيميائية للمركبات الجديدة باستخدام التقنيات الحسابية مثل دراسات ADME. حيث وجد ان كل المركبات التي تم انتاجها وفقا لهذه الدراسة تخضع لقاعدة ليبينسكي. تم استخدام مقياس التترازوليوم للزرعة الدقيقة (MTT) لتقييم فعالية المركبات المفحوصة مختبريا ضد خلايا سرطان الثدي البشري MDA-MB231. وظهرت نتائج الاختبار ان المركبين  $6^2$  بقيم  $\text{IC}_{50}$  تبلغ 47.78 و 111.8 ميكروغرام/مل على التوالي، كان لهما فعالية قوية مضادة للسرطان مقارنة مع الكركمين بقيمة  $\text{IC}_{50}$  تبلغ 125.5 ميكروغرام/مل.

**الكلمات المفتاحية:** الفعالية المضادة للسرطان، كركمين، قاعدة ليبينسكي، مقياس التترازوليوم للزرعة الدقيقة، الرنين الصوتي.